MAG3D and Its Application to Internal Flowfield Analysis

K. D. Lee[1], T. L. Henderson[2]
University of Illinois
Urbana, Illinois 61801

Y. K. Choo[3]
NASA Lewis Research Center
Cleveland, Ohio 44135

SUMMARY

MAG3D (Multi-block Adaptive Grid, 3D) is a three-dimensional solution-adaptive grid generation code which redistributes grid points to improve the accuracy of a flow solution without increasing the number of grid points. The code is applicable to structured grids with a multi-block topology. It is independent of the original grid generator and the flow solver. The code uses the coordinates of an initial grid and the flow solution on that grid to produce the coordinates of a solution-adapted grid and the flow solution interpolated onto the new grid. MAG3D uses a numerical mapping and potential theory to modify the grid distribution based on properties of the flow solution on the initial grid. In this paper, the adaptation technique is discussed, and the capability of MAG3D is demonstrated with several internal flow examples. Advantages of using solution-adaptive grids are also shown by comparing flow solutions on adapted grids with those on initial grids.

INTRODUCTION

The need for quality grids is increasing as the complexity in geometry and flow physics increases. The quality of a flow solution can be greatly enhanced by using a grid adapted to geometrical and physical features of the flow problem. Although some desirable grid characteristics can be accommodated in the initial grid generation process, it is difficult to generate a quality grid in a single step. In general, the grid must be supplied without *a priori* knowledge of the flow solution. This introduces the need for a solution-adaptive grid technique which couples the grid generation process with the flow solution process. Two approaches are available in generating solution-adaptive grids. One

---

[1]Associate Professor, Department of Aeronautical and Astronautical Engineering
[2]Graduate Research Assistant, Department of Mechanical Engineering
[3]Research Scientist, Internal Fluid Mechanics Division

approach is grid refinement which divides grid cells in regions of rapidly varying flow conditions into smaller cells, increasing the number of grid points. The other is grid redistribution which relocates grid points in an effort to distribute the truncation error more uniformly. Each method has advantages and disadvantages. The former seems more flexible but requires a provision in the flow solver to handle the grid change. The latter does not require any change to the flow solver but may degrade the grid quality. The MAG3D code is based on the grid redistribution technique.

The primary task of the solution-adaptive grid is to reduce the truncation error for improved solution accuracy. This is often achieved by controlling the cell size. However, there are other grid properties which strongly influence flow calculations. Therefore, a successful solution-adaptive grid should satisfy the following grid quality issues. It should not generate highly skewed cells, sharply kinked gridlines, or large cell aspect ratios, which tend to deteriorate the convergence rate and solution accuracy. Severe grid stretching and sudden change in cell size are also not desirable because they reduce the order of truncation. Better resolution can also be achieved if gridlines are aligned with flow characteristic lines such as a shock, a wake, a vortex core, and a contact discontinuity. Grid orthogonality is particularly important near the solid boundary for an efficient implementation of boundary conditions. In addition, there are other concerns: the grid adaptation process should be inexpensive compared to the flow calculation; it should be robust enough to handle different geometries and flow conditions; and, it should provide simple and predictable grid control options for the degree of adaptation and for the choice of grid quality.

METHOD

The adaptation method used in MAG3D is based on a numerical mapping and potential theory. It starts by defining numerical mapping functions of the initial grid into a parametric domain. The solution-adaptive grid generation is then a procedure of altering the mapping functions so that the flow gradients in the parametric domain become as uniform as possible. The mapping functions are modified by the influence of grid control sources whose strengths are defined from the distribution of flow variables on the initial grid. In two dimensions, the distribution of a flow variable over a grid forms a three-dimensional solution surface. Hence, the solution-adaptive grid generation in two dimensions can be compared to the surface grid generation on a three-dimensional surface patch. The difference lies in the source definition; the latter from the geometry and the former from the flow solution. Earlier, this technique was developed for geometry-adaptive surface grid generation [1]. It was later applied to solution-adaptive grid generation in two dimensions [2]. The present MAG3D code is an extension of the technique to three dimensions.

The present method of generating a solution-adaptive grid is as follows. First, the parametric representation of the initial grid is obtained by normalizing its computational coordinates, or indices. The result is a uniformly discretized cube in parametric coordinates, s_i, where i = 1,2,3 for each parametric direction. This mapping contains information about the initial grid which may already be tailored to the geometry and predicted flow

characteristics. Adaptation to the flow solution is performed by another mapping, which modifies the mapping functions using the influence of grid control sources. Grid control sources are defined separately for each parametric coordinate at the center of each cell in the parametric space. Source strengths are defined to reflect local solution characteristics on the initial grid. A monitor function, ϕ, is defined to be a linear combination of flow variables. In MAG3D, the source strengths are defined as a linear combination of the monitor function and its first- and second- derivative in each parametric coordinate. That is,

$$\sigma_i(Q) = w_{0_i}|\phi| + w_{1_i}\left|\frac{\partial \phi}{\partial s_i}\right| + w_{2_i}\left|\frac{\partial^2 \phi}{\partial s_i^2}\right| \qquad (1)$$

where Q stands for the source point. The w's are input parameters which allow for different weights to be placed on the various derivatives of ϕ in each parametric coordinate.

The second mapping includes the effects of all sources at every grid point in the parametric space. The source effects are defined as displacements, creating a modified set of parametric coordinates, $\hat{s}_i$,

$$\hat{s}_i(P) = s_i(P) + \sum_Q K_i(P,Q)\ \sigma_i(Q) \qquad (2)$$

where $K_i(P,Q)$ is the influence coefficient that determines the effect of a grid control source at a source point, Q, to a field point, P. It is defined from the potential theory as a function of the distance between the source point and the field point, given by

$$K_i(P,Q) = \left\{\sum_{i=1}^{3} \alpha_i (s_i(P) - s_i(Q))^2\right\}^{-1/2} \qquad (3)$$

where α_i is the weighting parameter in each parametric coordinate. The choice of weighting parameters determines the decay characteristics of the influence coefficient. The combination of the weights in (1) and the parameters in (3) defines the degree and character of the adaptation. The mapping also accounts for the effects of image sources which are defined as a reflection of the field sources across the domain boundaries. The use of image sources enforces the Newmann condition along a boundary, making the gridlines nearly orthogonal at the boundary. In a multi-block application, the image sources are obtained from the neighboring block in order to maintain the grid continuity across the block boundary.

The second mapping repels grid points away from strong sources. Therefore, cells containing strong sources become larger than those with weaker sources. Next, the modified parametric space is uniformly discretized. The points of this new discretization are then mapped back to the physical space by interpolating their locations from the known locations of points in the initial mapping. Since the modified parametric space is expanded

in regions of strong sources, the uniform rediscretization produces relatively fine grid spacing in these regions. In addition to the basic technology discussed here, MAG3D is equipped with many cost-saving features such as influence cut-off distance, group source influence, coarse grid adaptation, and multi-level searching algorithm.

The present adaptation technique has many advantages which stem from the use of parametric mapping and grid control source. For instance, basic characteristics of the initial grid can be retained while the grid is adapted to the flow solution. Linear potential theory allows for combined grid controls based on the superposition principle. The grid can be adapted to multiple flow quantities through a combined source definition. The adaptation can be performed only in a partial domain by defining the source strengths only in the region. The source formulation guarantees smoothness in the resulting grid, although sources are distributed irregularly. The method is not restricted to specific grid generators or flow solvers, and hence can be incorporated with many available grid and flow codes without modifications. The adaptation process can be repeated if a satisfactory result is not achieved after a single application.

DEMONSTRATIONS

The capability and merits of MAG3D are demonstrated with three flow problems shown in Figure 1: a supersonic corner flow, a supersonic injector nozzle flow, and a supersonic flow around a blunt fin mounted on flat plate. All flowfield calculations are performed using the CFL3D computer code acquired from the NASA Langley Research Center [3]. It solves the thin-layer, laminar, time-dependent, compressible, Reynolds-averaged Navier-Stokes equations using finite-volume, upwind-inviscid and centered-viscous discretization, factored-implicit integration, and multi-grid acceleration. The test cases are selected because the flowfields contain many flow features which are suitable for grid adaptation, such as shocks, mixing layers, shock-shock and shock-boundary-layer interactions. The sensitivity of these flow features to grid quality demonstrates the effectiveness of the solution-adaptive grid in improving solution accuracy. In all three cases, the grid control sources are defined as a combination of gradients of the Mach number and pressure on the initial grid. This choice for the monitor function performs well in adapting the grid to both shocks and boundary layers.

The first example is the supersonic, symmetric corner flow bounded by the intersection of two wedges with equal angles of 9.5 degrees as shown in Figure 1 [4]. A no-slip condition is imposed on the wedge surfaces on the bottom and right sides and a symmetric condition is used on the other two sides. Laminar flow is considered, with a free stream Mach number of 3.0 and a Reynolds number of 3.07×10^6 per unit length. The calculations are performed on 33x65x65 grids. In order to observe the capability of MAG3D, the adaptations are performed with directional applications by the choice of w's in (1). The grids and flow solutions are shown in Figures 2 to 5 for the initial grid and 1D, 2D, and 3D adaptations, respectively. In grid pictures, every other gridline is shown for clarity. Here,

the 1D adaptation means that the grid is adapted only in one parametric coordinate direction. The 2D adaptation stands for the adaptation in two coordinate directions. However, the source influences are always accounted for in all three directions. These tests demonstrate the controllability of MAG3D. More global adaptation is possible by changing α_i in (3). It is noteworthy that the gridlines become near orthogonal to the boundaries due to the use of image sources. As expected, the adapted grids produce a much better shock structure and a better resolution for the shock-induced recirculation zone in the boundary layer.

The second problem is a supersonic mixing nozzle flow where a sonic transverse jet is injected into a Mach 4 freestream [5]. Only the perfect gas model is considered; no chemistry is included. The geometry and the flow conditions are shown in Figure 1. No-slip and adiabatic conditions are imposed on the top wall where the jet is located. Symmetric boundary conditions are used at the bottom wall and both side walls. At the exit, the no flow-gradient condition is applied. The grid size is 49x33x33. The initial grid is already clustered to resolve the jet and the wall boundary layer. The grid and the flow solutions are compared for the initial and solution-adapted grids in Figures 6 and 7, respectively. Again, only every other line is shown for clarity. It can be seen that the gridlines of the adapted grid follow the bow shock and the mixing layer. Improved resolution can be observed with the solution-adaptive grid: the bow shock becomes sharper, and the temperature mixing layer is captured more clearly.

The third example is the supersonic flow field around a blunt fin mounted on a flat plate as shown in Figure 1 [6]. This flow contains a complex three-dimensional shock-wave and boundary-layer interaction. The free stream conditions are Mach number of 2.95 and Reynolds number of 3 million based on the fin width. The grid size is 65x33x33. The initial grid is clustered in the boundary layers along the flat plate and the fin surface. The boundary layer on the plate is assumed to start at the upstream far-field boundary. Figures 8 and 9 show the grids and flow solutions for the initial and adapted grid cases respectively. The solution-adaptive grid shows the grid clustering in the shock and shear layer regions. Therefore, sharper shocks and shear layers can be observed in front of the blunt fin.

In order to compare the convergence rate, flow calculations on the solution-adaptive grids are started from the free stream condition instead of the interpolated solutions from MAG3D. In all three cases, the solution-adaptive grids do not significantly deteriorate the convergence rate of the flow solver. The solution-adaptive grids demonstrate a significant improvement in the resolution of major flow features obtained with the initial grids. The solution-adaptive grid not only improves the sharpness of the flow solution, but also captures important secondary flow structures that are not presented in the initial solutions.

CONCLUDING REMARKS

MAG3D is shown as an effective tool to generate solution-adaptive grids for various three-dimensional flow problems. The presented adaptation technique is an efficient

method to improve certain grid properties. The method is convenient because it does not require any modifications to grid generators and flow solvers. Also, it can preserve the basic grid characteristics of the initial grid, which is often desirable in practical applications. The degree and locality of adaptation can be controlled in each direction separately through input parameters. Repeated adaptation can be performed when single adaptation is not satisfactory. The presented examples show that the solution-adapted grid significantly improves the flow resolution with little penalty in convergence and stability in the flow calculation.

In some applications, solution-adaptive grids may possess undesirable grid properties such as severe grid distortion and sudden grid stretching. Therefore, a grid-quality assessment and manipulation process will be incorporated into MAG3D to help prevent undesirable grid properties. The same adaptation technique can be utilized for the grid quality enhancement [7]. In this case, the grid control sources are extracted from the distribution of grid quality measures such as skewness and cell aspect ratio.

REFERENCES

1. Lee, K. D. and Loellbach, J. M., "Geometry-Adaptive Surface Grid Generation Using Parametric Projection," Journal of Aircraft, Vol. 26, No. 2, pp. 162-167, February 1989.

2. Lee, K. D. And Loellbach, J. M., "A Mapping Technique for Solution-Adaptive Grid Control," Proceedings AIAA 7th Aerodynamics Conference, Seattle, WA, pp. 129-139, AIAA Paper 89-2178, 1989.

3. Vatsa, V., Thomas, J. L. and Wedan, B. W., "Navier-Stokes Computations of Prolate Spheroids at Angle of Attack," AIAA Paper 87-2627-CP, 1987.

4. West, J. E. and Korkegi, R. H., "Supersonic Interaction in the Corner of Intersecting Wedges at High Reynolds Numbers," AIAA Journal, Vol. 10, No. 5, pp. 652-656, May 1972.

5. Yu, S. T., Tsai, Y. P., and Shuen, J. S., "Three-Dimensional Calculation of Supersonic Reacting Flows Using an LU Scheme," AIAA Paper 89-0391, 1989.

6. Nakahashi, K. and Deiwert, G. S., "A Three-Dimensional Adaptive Grid Method," AIAA Paper 85-0486, 1985.

7. Lee, K. D., Henderson, T. L., and Choo, Y. K., "Grid Quality Improvement by a Grid Adaptation Technique," Proceedings 3rd International Conference on Numerical Grid Generation in Computational Fluid Dynamics and Related Fields, Barcelona, Spain, pp. 597-606, June 1991.

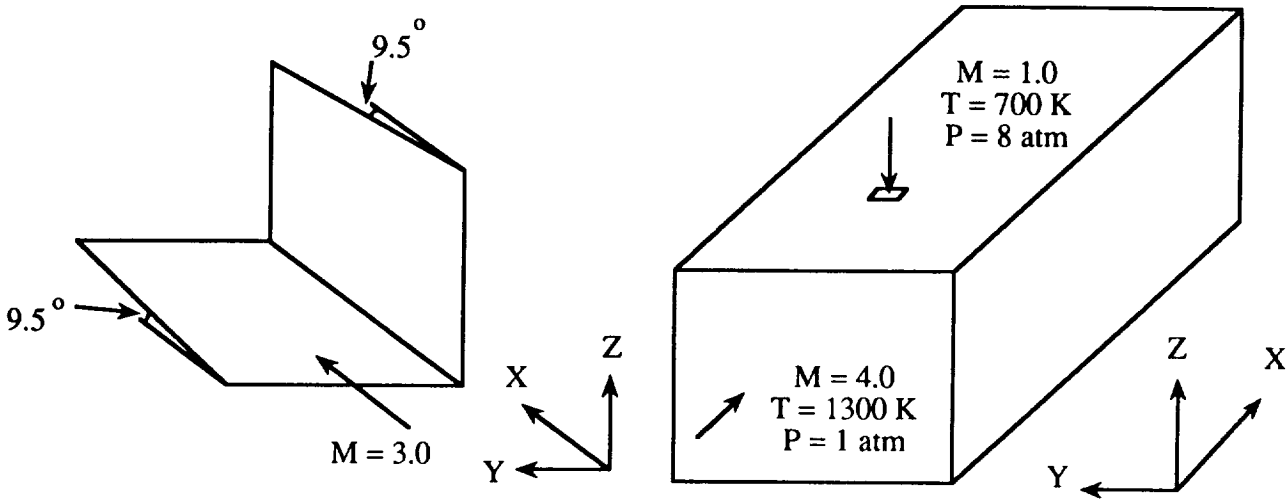

(a) Supersonic 3D corner flow.

(b) Supersonic mixing with transverse jet.

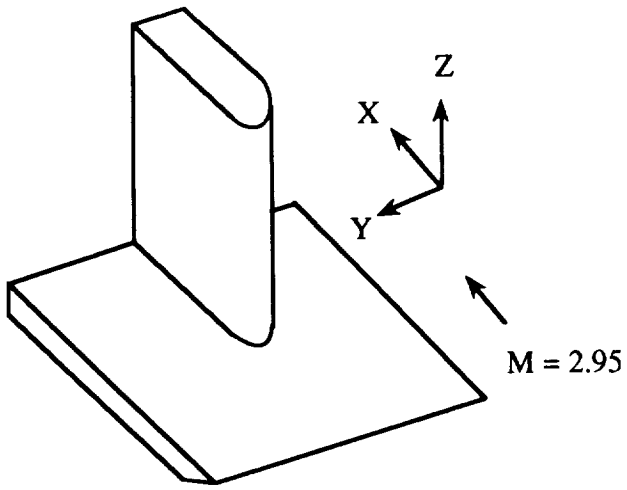

(c) Supersonic flow over blunt fin on flat plate.

Figure 1. Schematic flow configurations of the model problems.

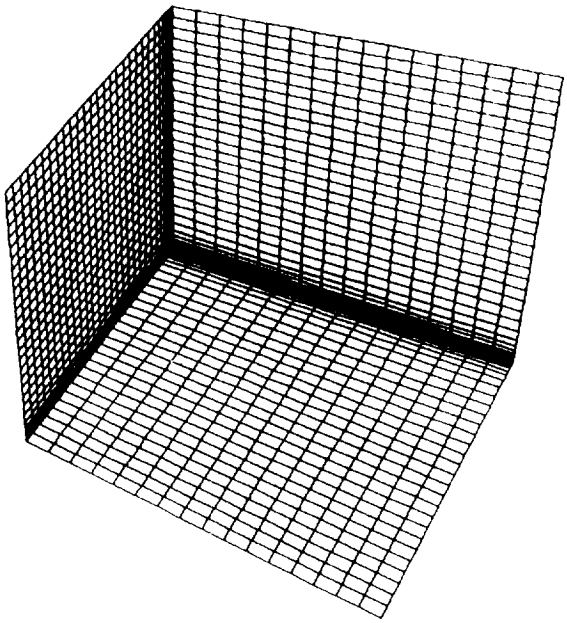

(a) Initial grid.

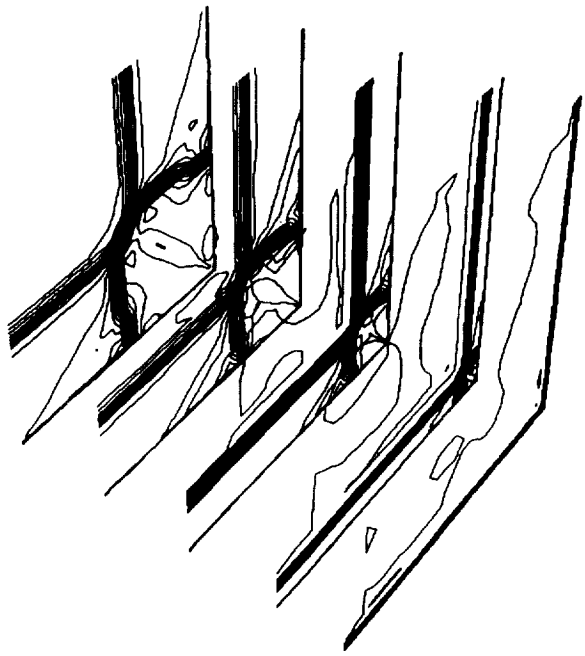

(b) Density contours on i-planes.

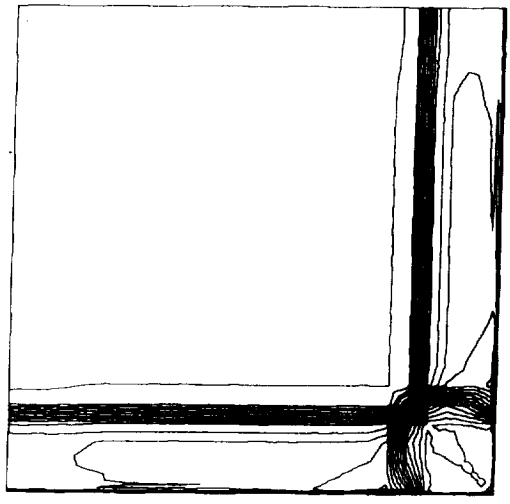

(c) Density contours at an i-plane.

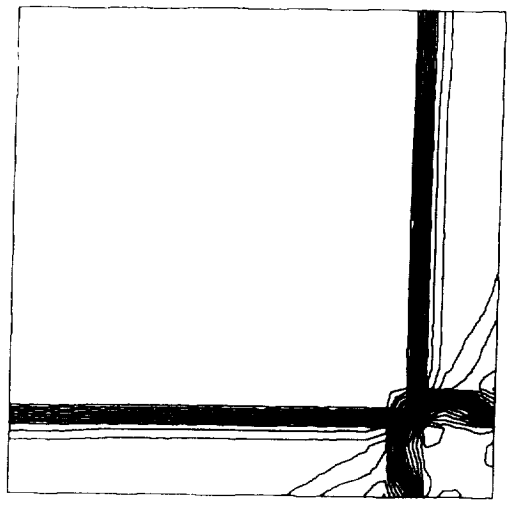

(d) Pressure contours at an i-plane.

Figure 2. Initial grid and its flow solutions - supersonic 3D corner flow.

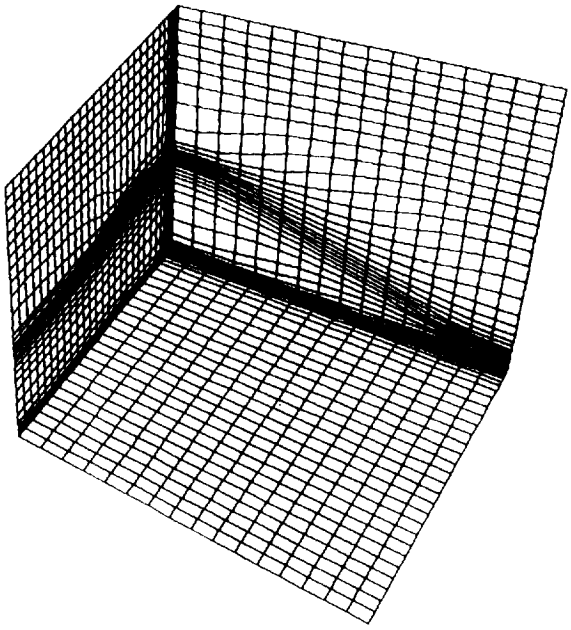

(a) One-direction adapted grid.

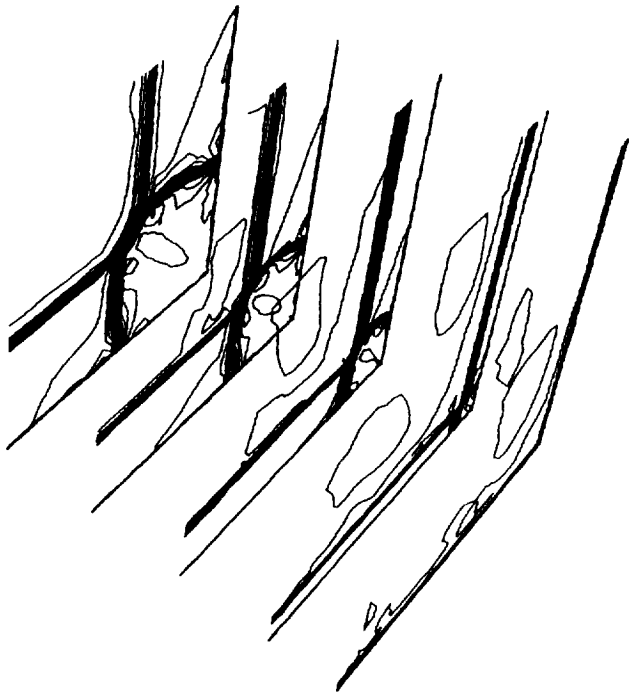

(b) Density contours on i-planes.

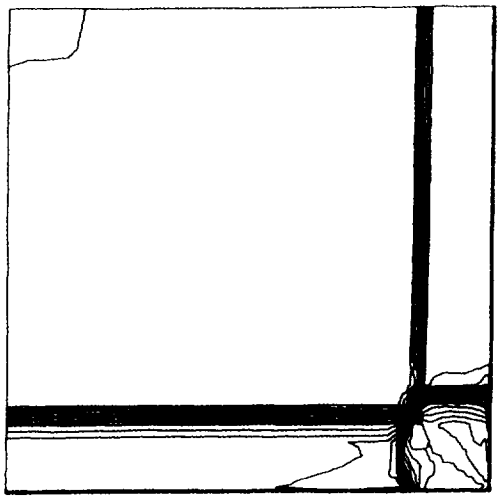

(c) Density contours at an i-plane.

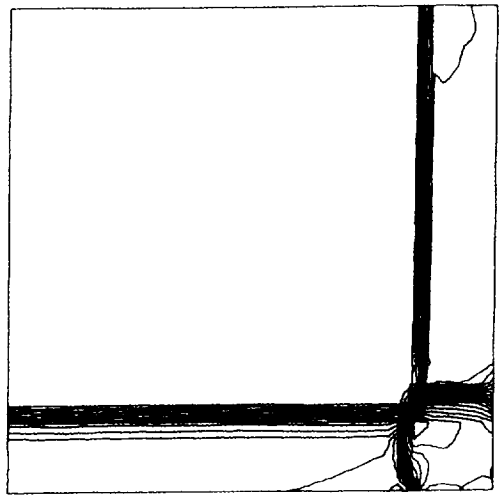

(d) Pressure contours at an i-plane.

Figure 3. One-direction adapted grid and its flow solutions - supersonic 3D corner flow.

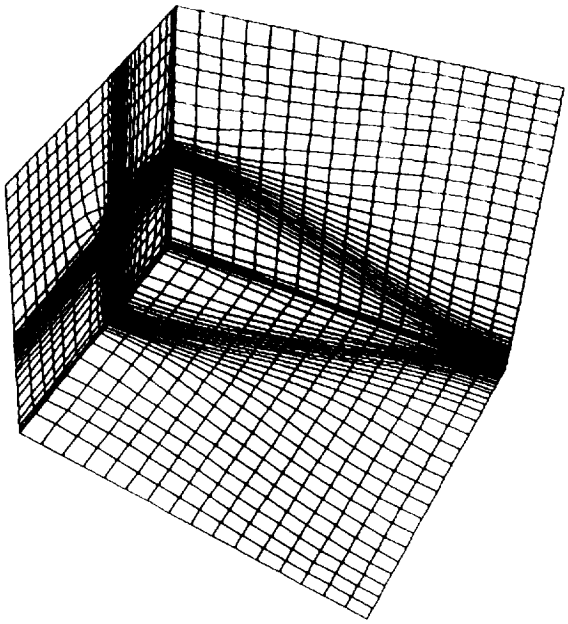

(a) Two-direction adapted grid.

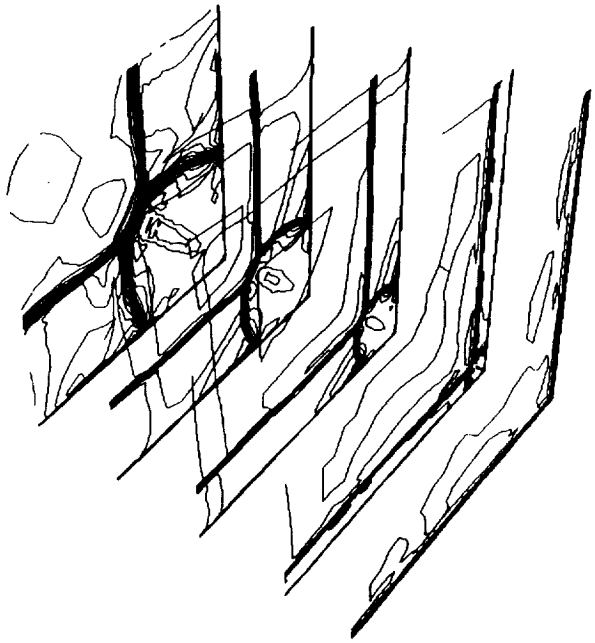

(b) Density contours on i-planes.

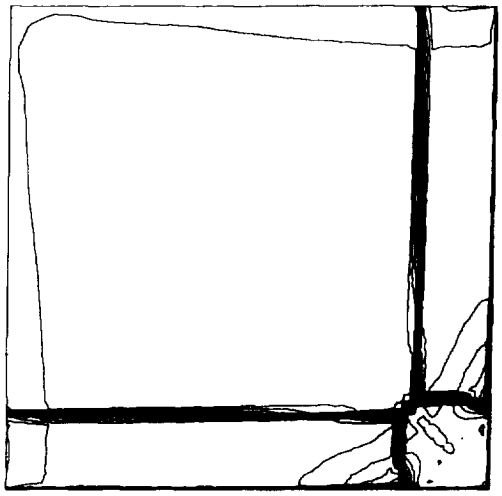

(c) Density contours at an i-plane.

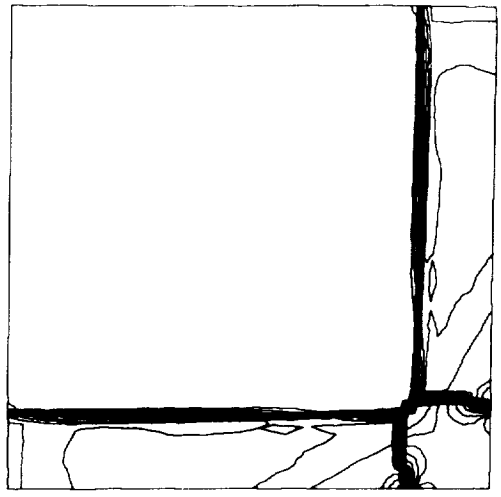

(d) Pressure contours at an i-plane.

Figure 4. Two-direction adapted grid and its flow solutions - supersonic 3D corner flow.

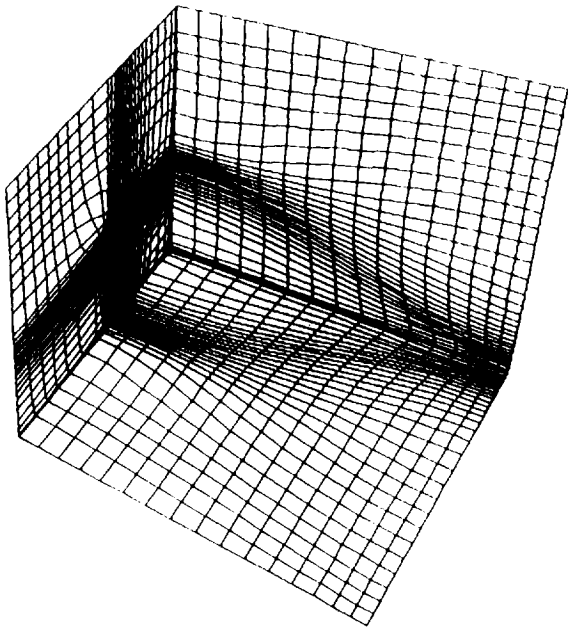

(a) Three-direction adapted grid.

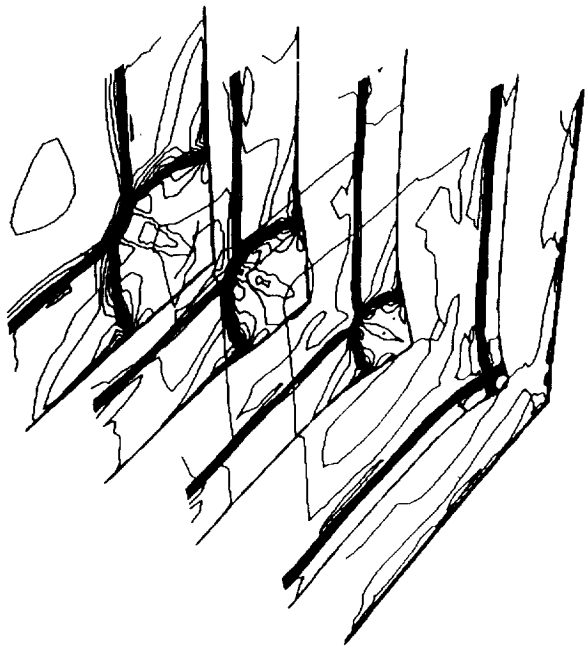

(b) Density contours on i-planes.

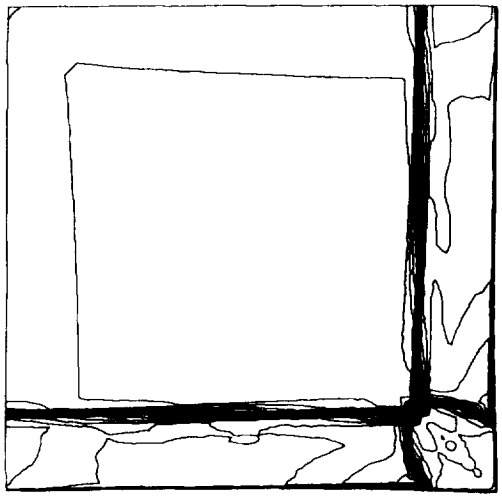

(c) Density contours at an i-plane.

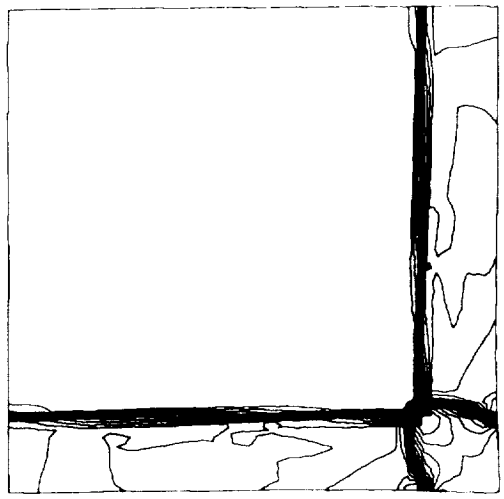

(d) Pressure contours at an i-plane.

Figure 5. Three-direction adapted grid and its flow solutions - supersonic 3D corner flow.

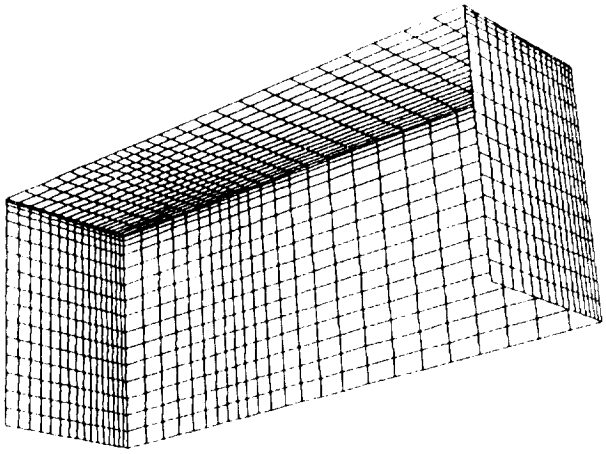

(a) Initial grid.

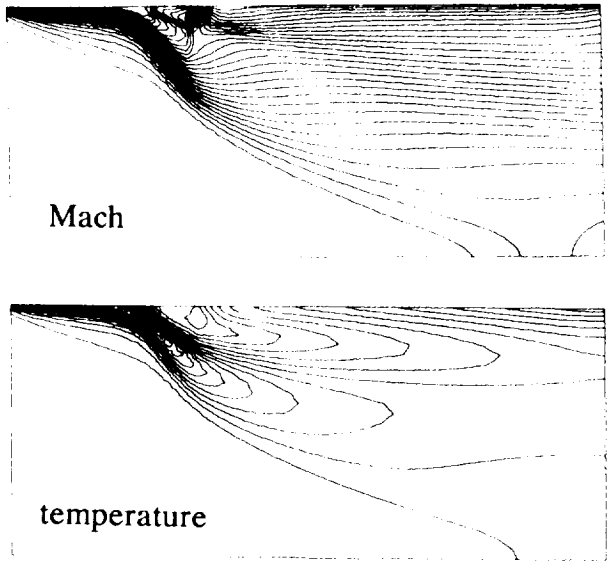

(b) Mach and temperature contours on the symmetry plane.

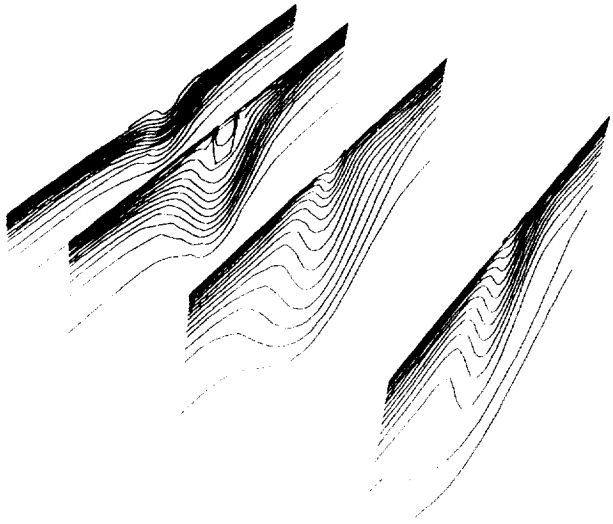

(c) Mach contours at i-planes.

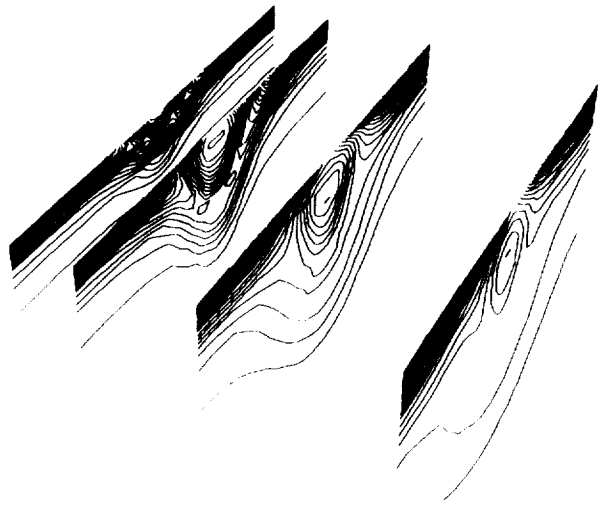

(d) Temperature contours at i-planes.

Figure 6. Initial grid and its flow solutions - supersonic mixing with a transverse jet.

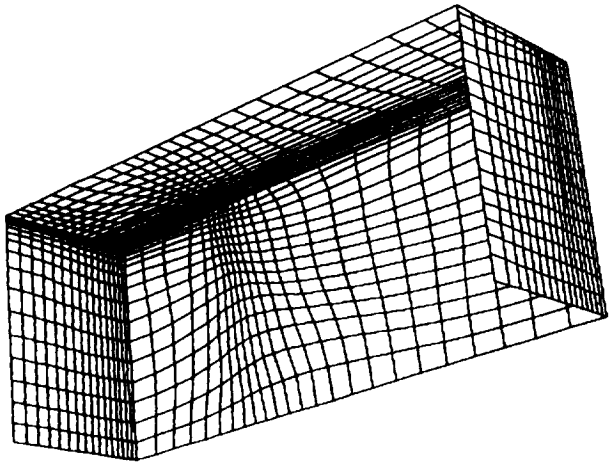

(a) Adapted grid.

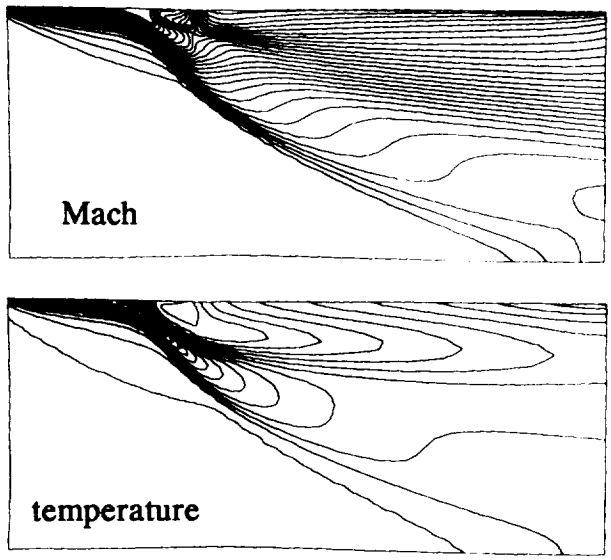

(b) Mach and temperature contours on the symmetry plane.

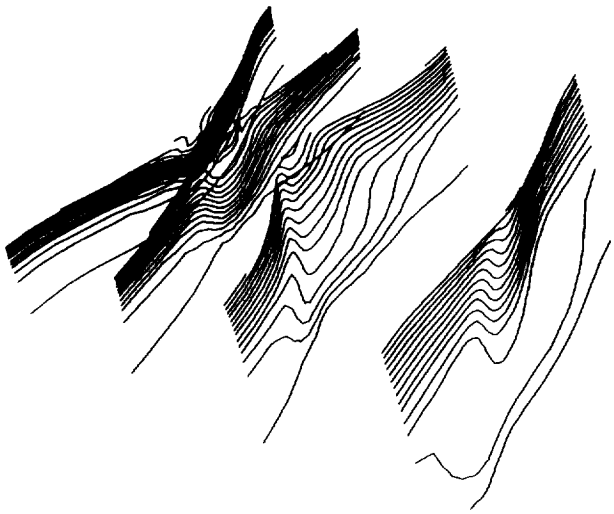

(c) Mach contours at i-planes.

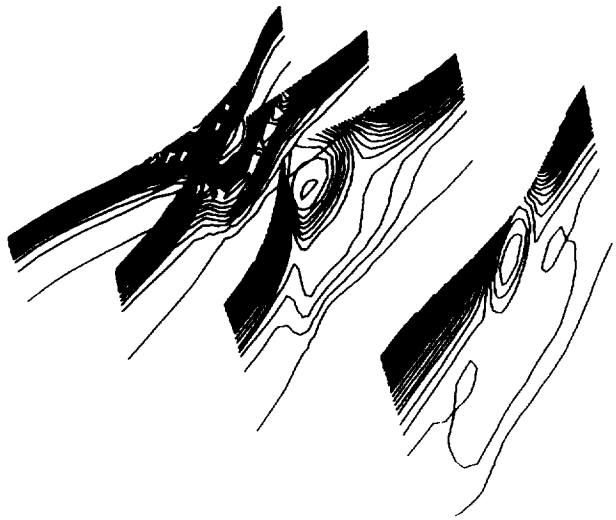

(d) Temperature contours at i-planes.

Figure 7. Adapted grid and its flow solutions - supersonic mixing with a transverse jet.

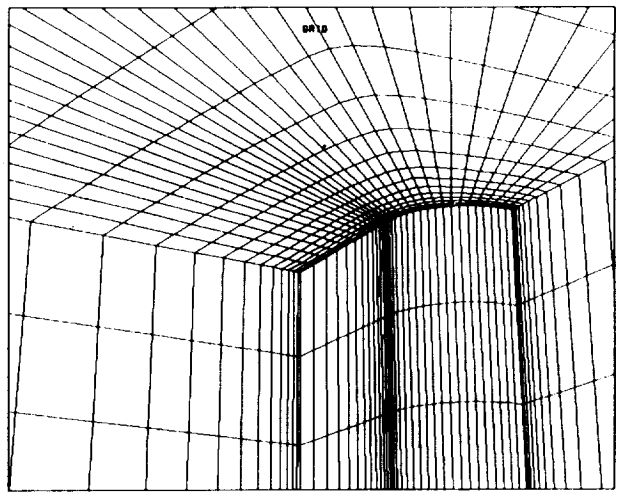

(a) Initial grid - upper side.

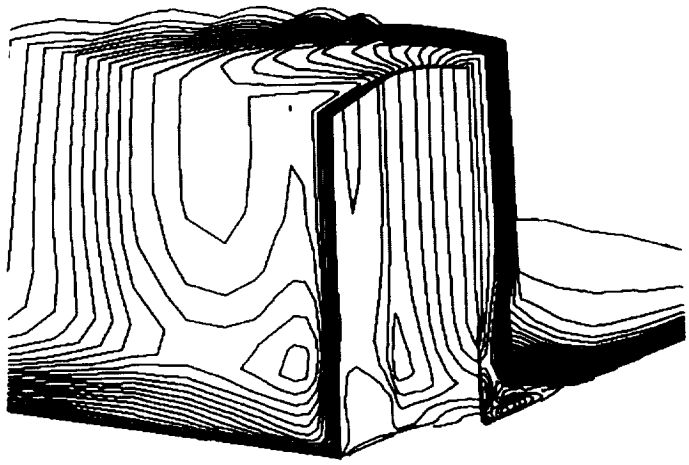

(b) Mach contours on grid in (a).

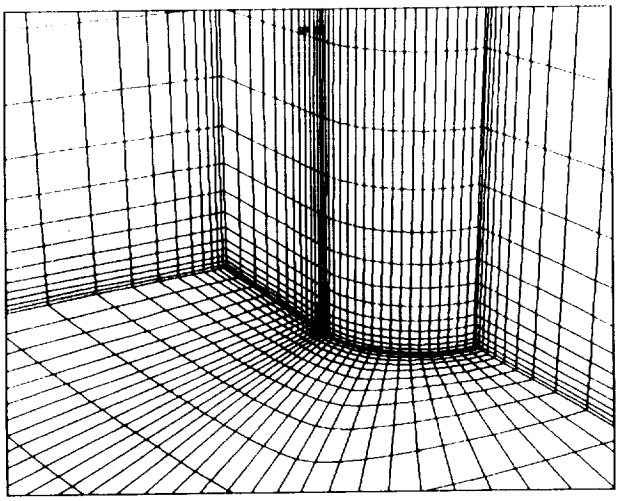

(c) Initial grid - lower side.

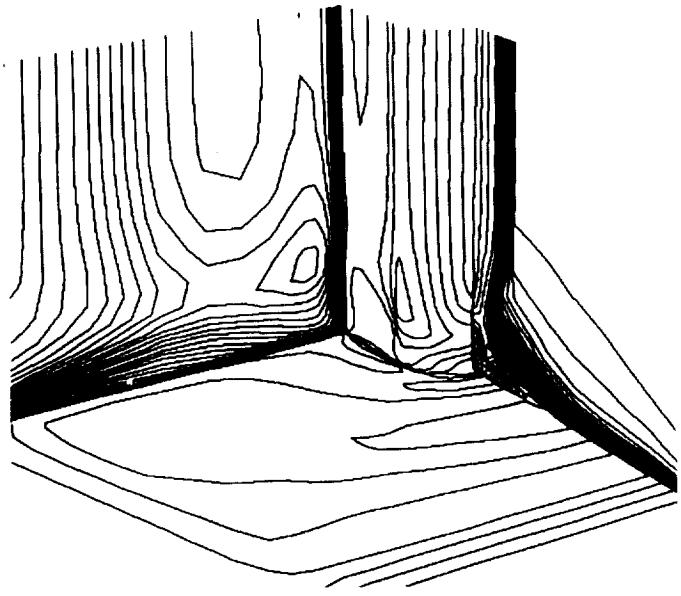

(d) Mach contours on grid in (c).

Figure 8. Initial grid and its flow solutions - supersonic flow over a blunt fin on a flat plate.

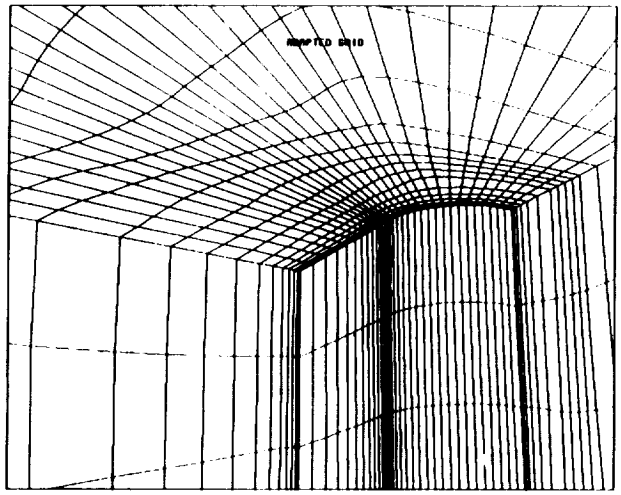

(a) Adapted grid - upper side.

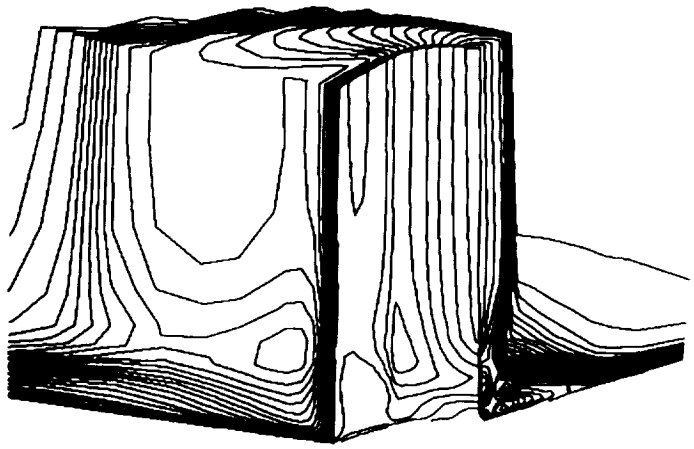

(b) Mach contours on grid in (a).

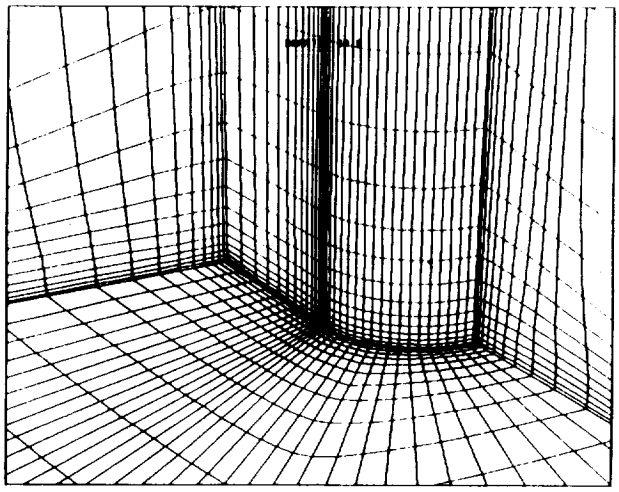

(c) Adapted grid - lower side.

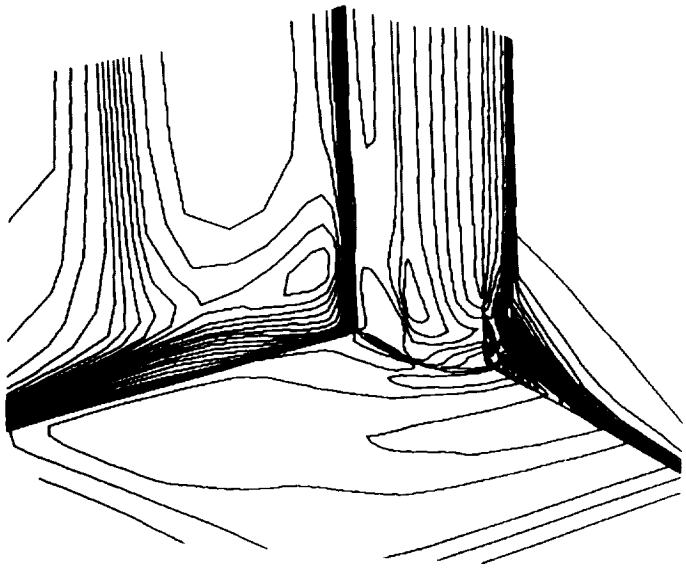

(d) Mach contours on grid in (c).

Figure 9. Solution-adaptive grid and its flow solutions - supersonic flow over a blunt fin on a flat plate.